

## RESEARCH LETTER

10.1002/2016GL068059

## Key Points:

- Hypothesized causality of midlatitude hot summer originating from ice loss is not supported
- Arctic ice loss has induced significant summer midlatitude cooling trends of SAT
- Increasing greenhouse gas and SST warming outside the Arctic explains observed trends

## Supporting Information:

- Supporting Information S1

## Correspondence to:

Q. Wu,  
qigangwu@nju.edu.cn

## Citation:

Wu, Q., L. Cheng, D. Chan, Y. Yao, H. Hu, and Y. Yao (2016), Suppressed midlatitude summer atmospheric warming by Arctic sea ice loss during 1979–2012, *Geophys. Res. Lett.*, 43, 2792–2800, doi:10.1002/2016GL068059.

Received 1 FEB 2016

Accepted 29 FEB 2016

Accepted article online 4 MAR 2016

Published online 18 MAR 2016

## Suppressed midlatitude summer atmospheric warming by Arctic sea ice loss during 1979–2012

Qigang Wu<sup>1</sup>, Luyao Cheng<sup>1</sup>, Duo Chan<sup>1</sup>, Yonghong Yao<sup>1</sup>, Haibo Hu<sup>1</sup>, and Ying Yao<sup>1</sup>
<sup>1</sup>School of Atmospheric Science, Nanjing University, Nanjing, China

**Abstract** Since the 1980s, rapid Arctic warming, sea ice decline, and weakening summer circulation have coincided with an increasing number of extreme heat waves and other destructive weather events in the Northern Hemisphere (NH) midlatitudes in summer. Recent papers disagree about whether such high-impact events are related to Arctic warming and/or ice loss. Here we use atmospheric model ensemble simulations to attribute effects of sea ice loss and other factors on observed summer climate trends during 1979–2012. The ongoing greenhouse gas buildup and resulting sea surface temperature warming outside the Arctic explains nearly all land warming and a significant portion of observed weakening zonal winds in the NH midlatitudes. However, sea ice loss has induced a negative Arctic Oscillation(AO)-type circulation with significant summer surface and tropospheric cooling trends over large portions of the NH midlatitudes, which reduce the warming and might reduce the probability of regional severe hot summers.

## 1. Introduction

A topic of increasing interest is whether Arctic warming and sea ice loss induces midlatitude cold spells and heat waves via changes in the large-scale circulation [Francis and Vavrus, 2012, 2015; Cohen et al., 2014; Barnes, 2013; Barnes et al., 2014; Wallace et al., 2014; Trenberth et al., 2014; Overland, 2014]. During recent decades, surface and atmospheric warming has been larger over the Arctic than at other latitudes, a phenomenon called Arctic amplification [Serreze et al., 2009; Stroeve et al., 2012]. The summer and autumn sea ice extent in 1979–2012 has declined at a rate of about 6–7% per decade [Vaughan et al., 2014]. Arctic sea ice loss contributes to Arctic amplification through a positive ice-albedo feedback, where the exposed ocean absorbs more solar radiation, leading to further warming [Serreze et al., 2009]. Along with these Arctic changes, many midlatitude NH land regions have experienced both frequent anomalously cold and snowy winters and record-breaking summer heat waves [Coumou and Rahmstorf, 2012; Coumou et al., 2014]. The NH midlatitude summer circulation has significantly weakened with a long-term decline in eddy kinetic energy and zonal mean zonal wind since 1979 [Coumou et al., 2015]. A reduced midlatitude zonal wind speed is associated with a more meridional flow and a slower eastward progression of upper level large-scale Rossby waves [Palmén and Newton, 1969], which is hypothesized to make weather more persistent and hence favors the occurrence of prolonged extreme weather events [Francis and Vavrus, 2012; Coumou et al., 2014, 2015].

Most previous studies of linkages between the Arctic and midlatitude climate have focused on winter and suggest that ongoing Arctic sea ice loss is related to warming around the Arctic, but the sea ice loss may also remotely enhance both cold and mild winter extremes in NH midlatitudes [Francis et al. [2009], Overland and Wang [2010], Wu and Zhang [2010], Strong et al. [2010], Magnusdottir et al. [2004], Honda et al. [2009], Liu et al. [2012], Orsolini et al. [2012], Screen et al. [2013], Kim et al. [2014], Peings and Magnusdottir [2014], Screen et al. [2014], and many others], although there are many disagreements about mechanisms and regional impacts [Cohen et al., 2014; Barnes and Screen, 2015]. Recent observational studies have also hypothesized that in the summer, sea ice loss and Arctic amplification cause more frequent extreme midlatitude heat events by weakening the poleward temperature gradient, which induces circulation changes such as reduced zonal winds and increased wave amplitudes [Francis and Vavrus, 2012, 2015; Overland, 2014; Coumou et al., 2014, 2015; Petoukhov et al., 2013; Tang et al., 2014]. Such hypothesized linkage is based on the observed coincidence of events, trends, or statistical correlations, so the chain of cause and effect is not clear. A strong simultaneous connection between sea ice and midlatitude atmospheric fields can be alternatively explained as the response of sea ice extent anomalies to changing temperature and atmospheric circulation, instead as feedbacks of sea ice retreat onto the atmospheric circulation, since the interaction between atmosphere and sea ice is dominantly characterized by atmospheric forcing on Arctic sea ice anomalies in summer and other seasons

[Wu and Zhang, 2010]. The observed lagged relationship between the summer mean surface air temperature (SAT) and the spring bimonthly April–May mean sea ice extent index shows a significant cooling response to early-season Arctic sea ice loss over large midlatitude areas of northern continents (Figure S1 in the supporting information).

The hypothesis that Arctic sea ice loss remotely causes more frequent extreme hot midlatitude summer weather is not confirmed in modeling studies and has instead often been criticized [Barnes, 2013; Barnes *et al.*, 2014; Wallace *et al.*, 2014; Trenberth *et al.*, 2014]. Such links are not robust across other observational studies [Barnes, 2013; Barnes *et al.*, 2014], and random internal variability might obscure a possible link between sea ice changes and midlatitude weather [Barnes, 2013; Screen *et al.*, 2014]. For example, recent climate anomalies such as hot midlatitude summers may simply be due to natural large-scale atmospheric circulation variations [Wallace *et al.*, 2014]. Trenberth *et al.* [2014] argue that the Arctic has little effect on the midlatitude circulation because Arctic precipitation changes cause much smaller latent heat anomalies than typical variations in the tropics. Due to the ongoing controversies, this study analyzes a large ensemble of simulations covering 1979–2012 to examine the likely summer impacts of observed Arctic sea ice loss on the midlatitudes.

## 2. Data and Methodology

Observed SAT is obtained from the NOAA “Merged Air Land and sea surface temperature (SST) Anomalies” data set [Smith *et al.*, 2008] for 1979–2012 on a 5° latitude-longitude grid. Only grid boxes having more than 66% of years available are included in the trend analysis. Observed changes in tropospheric air temperature, geopotential height, and zonal and meridional wind fields are estimated from the ERA-Interim reanalysis [Dee *et al.*, 2011]. Since the simulation outputs are defined at a higher horizontal resolution than the observed SAT or ERA-Interim reanalysis atmospheric fields, all observed and simulated data sets are averaged onto a 5° latitude-longitude grid for the analysis.

Here we examine summer atmospheric responses to Arctic sea ice loss by analyzing a large ensemble of simulations, covering 1979–2012, from the Community Atmosphere Model 4.0 (CAM4) [Neale *et al.*, 2013] and European Centre/Hamburg version 5 (ECHAM5) [Roeckner *et al.*, 2003] atmospheric models, performed by NOAA Earth System Research Laboratory (ESRL) [Perlwitz *et al.*, 2015]. Table S1 gives an overview of two large ensemble experiments designed to investigate effects of Arctic sea ice loss. These are Atmospheric Modeling Intercomparison Project (AMIP) simulations using prescribed monthly spatial fields of SST and sea ice concentration (SIC). Set 1 model runs (20 CAM4 and 30 ECHAM5 ensemble members) are forced by observed greenhouse gas (GHG) concentrations, SST, and sea ice concentration (SIC). Set 2 model runs (20 CAM4 and 10 ECHAM5) use the same GHG and SST data but remove the effect of sea ice loss by repeating the 1979–1988 climate average cycle of SIC (and SST in grid boxes partly covered by sea ice) in each year. Since observed changes in Arctic SST and sea ice may be correlated, the set 2 experiment setup enables the response to ice loss to be removed but discounts the response to the direct SST changes due to the Arctic ocean warming in the sea ice margin, which might influence the response. For most analyses, simulations from both models are combined to form a superensemble called AMIP\_full for the 50 runs from set 1 or AMIP\_noSIC for the 30 set 2 runs. A superensemble mean field provides an estimate of the atmospheric response to a specific forcing combination.

The specific atmospheric response attributed to forcing from Arctic sea ice changes (referred to as AMIP\_SIC) in these models is the AMIP\_full minus AMIP\_noSIC superensemble mean difference. In contrast to previous modeling studies which run simulations forced by general sea ice trends or case studies that compare years with large opposite sea ice anomalies [e.g., Peings and Magnusdottir, 2014; Screen *et al.*, 2014; Balmaseda *et al.*, 2010; Petrie *et al.*, 2015], these simulations are designed to better isolate the specific atmospheric responses to ongoing observed Arctic sea ice losses [Screen *et al.*, 2013; Perlwitz *et al.*, 2015]. Following analyses use superensemble averages and focus on 1979–2012 forced linear trends of atmospheric fields in June–July–August (JJA). The climate response is measured alternatively by “epoch differences” between the means of the latest 10 JJA periods (2003–2012) and the first 10 JJA periods (1979–1988). The two methods yield virtually identical results (Figure S2).

For significance testing, we compute the standard deviation ( $\sigma$ ) of 34 year trends in any region or grid box using the 80 superensemble members of AMIP\_full and AMIP\_noSIC runs, with all members assumed to be independent. The same  $\sigma$  values are assumed to apply when evaluating significance of differences from zero of an observed or reanalysis trend (e.g., Figures 1a, 3a, and 3b) or differences of a model trend from

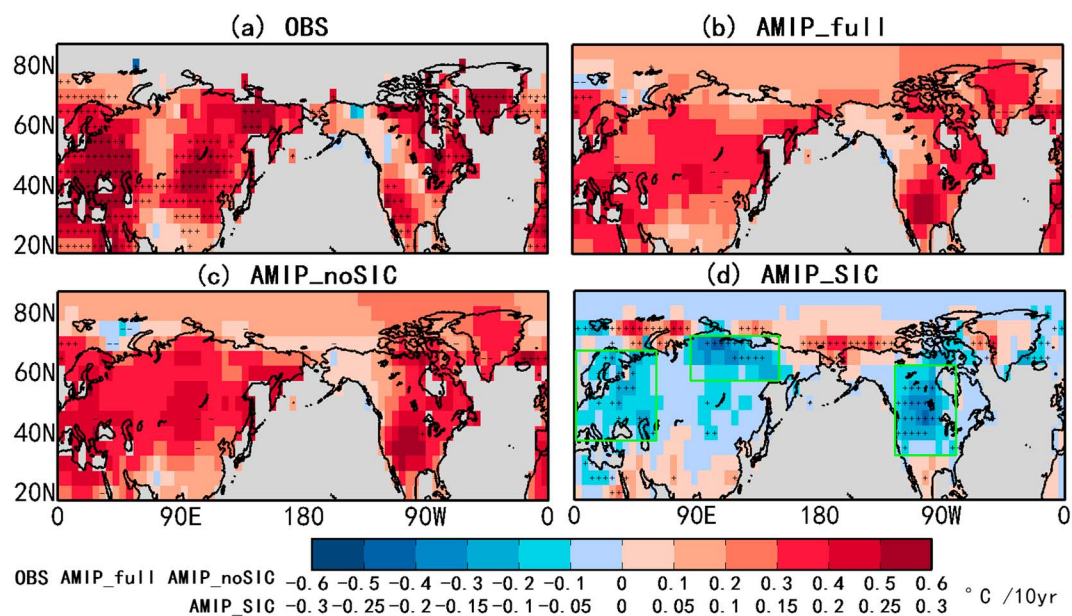


**Figure 1.** The 1979–2012 summer (JJA) linear SAT trends [ $\text{K} (10 \text{ yr})^{-1}$ ]. (a) From observed NOAA data set. (b–d) Superensemble mean (average of all CAM4 and ECHAM5 simulations) trends from (Figure 1b) AMIP\_full, (Figure 1c) AMIP\_noSIC runs, and (Figure 1d) attributed to sea ice forcing, AMIP\_SIC. Gray shaded areas indicate insufficient data in Figure 1a and oceans outside the Arctic in all panels. Plus/minus symbols mark individual grid boxes with significant warming/cooling trends in Figure 1a, significantly larger/smaller forced trends than observations in Figures 1b and 1c, and significantly different forced trends between the AMIP\_full and AMIP\_noSIC experiments in Figure 1d, all at the 5% significance level. Three green rectangles in Figure 1d outline areas with most significant cooling trends used in Figure 2.

the corresponding observed or reanalysis trend (e.g., Figures 1b, 1c, and 3c–3f). Last, we assess statistical significance of the grid box responses to sea ice forcing using a standard two-tailed difference of means Student's  $t$  test. More details of the significance test can be found in the supporting information.

### 3. Results

In observation data, significant JJA warming trends occurred in most parts of North America and northern Eurasia (Figure 1a). AMIP\_full and AMIP\_noSIC simulations (Figures 1b and 1c) reproduce the observed general land warming pattern moderately well, and very few land grid boxes (with sufficient observations) have observed and superensemble trends significantly different at the 5% level. Figure 1d shows that the isolated warming effect of observed sea ice loss is statistically significant only in small regions collocated with the greatest sea ice losses just north of Eurasia to western Canada. Sea ice loss is also associated with mostly insignificant warming (less than  $0.05^\circ\text{C}/10 \text{ yr}$ ) south of  $35^\circ\text{N}$ , but larger areas of significant cooling in Eurasia and western North America partly offset SAT warming caused by other forcings. Figure 2 further shows that in the three areas with most significant cooling trends outlined in Figure 1d, SAT trends from simulations that include SST and prescribed radiative forcings are clearly different from trends resulting only from sea ice changes. In each region, the cooling trend due to SIC forcing (from  $-0.07$  to  $-0.11^\circ\text{C}/10 \text{ yr}$ ) offsets about 20–30% of warming in the AMIP\_noSIC experiment, implying that if Arctic sea ice had not diminished, midlatitude warming would have been even stronger.

In the troposphere, observed deep warming responses at 925 and 500 hPa based on the ERA-Interim reanalysis (Figures 3a and 3b) are moderately well simulated by forcings included in the AMIP\_full and AMIP\_noSIC runs, especially over midlatitude land areas (Figures 3c–3f). However, trends differ for several reasons: First, both AMIP simulation experiments omit certain other anthropogenic forcings, such as changes in land use, land cover, and carbon aerosols, which might have had regionally varying effects on the actual trend since 1979. Second, the ensemble averaging process filters out most natural internal variability simulated by individual runs. This is shown in Figures 2a, 2c, and 2e by larger annual observed fluctuations than in the ensemble mean model simulations. Finally, AMIP simulations do not allow the atmosphere and ocean to act as an interactive, coupled system, which may affect some aspects of the atmosphere's response to sea ice loss [Deser et al., 2015].

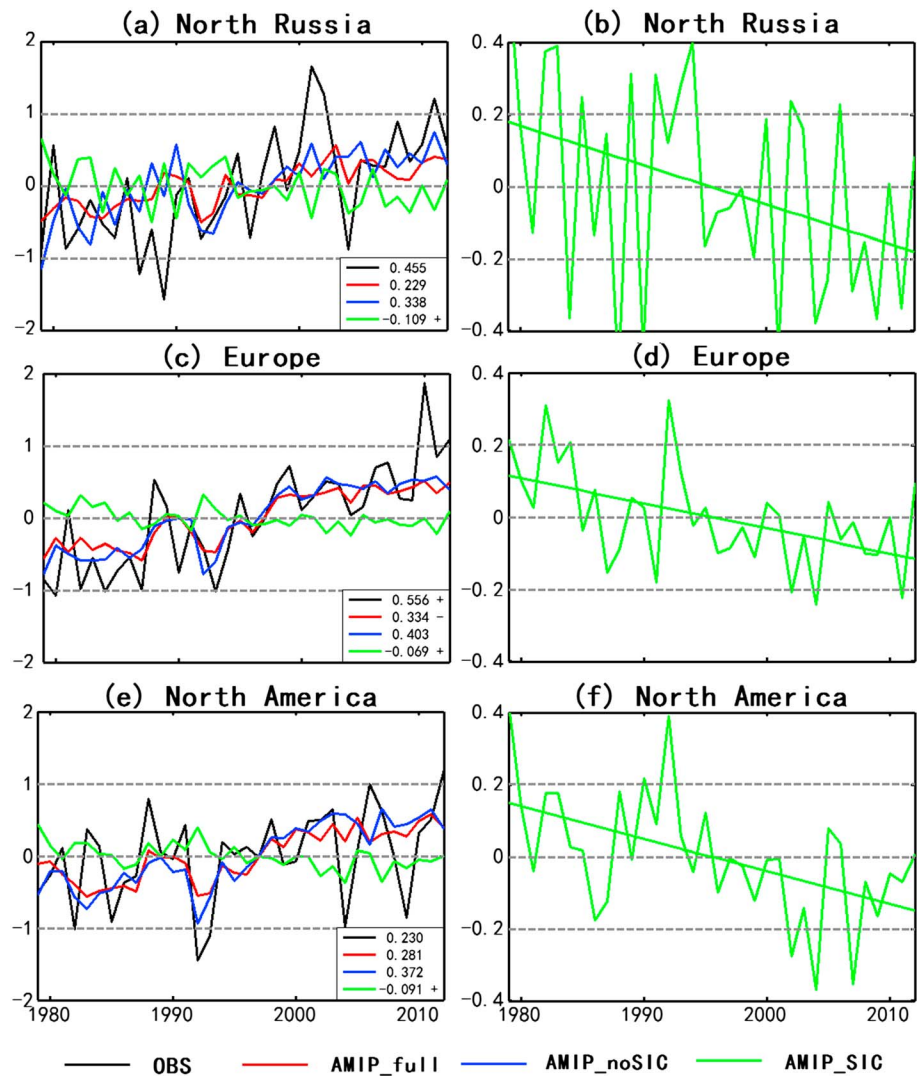


**Figure 2.** Time series of anomalous summer (JJA) areal averaged SAT and the corresponding linear trends [ $K (10 \text{ yr})^{-1}$ ] for 1979–2012 over three regions indicated with green rectangles in Figure 1d including (a, b) North Russia ( $60^{\circ}$ – $75^{\circ}\text{N}$ ,  $85^{\circ}$ – $150^{\circ}\text{E}$ ), (c, d) Europe ( $40^{\circ}$ – $70^{\circ}\text{N}$ ,  $0^{\circ}$ – $60^{\circ}\text{E}$ ), and (e, f) North America ( $35^{\circ}$ – $65^{\circ}\text{N}$ ,  $80^{\circ}$ – $125^{\circ}\text{W}$ ) in (thick black line) the observed data set, the superensemble mean from the (red) AMIP\_full or (blue) AMIP\_noSIC experiments, and (green) attributed to sea ice forcing, AMIP\_SIC. Plus/minus symbols by linear trends in Figures 2a, 2c, and 2e have the same meanings as in Figure 1a for an observed trend (black line), Figures 1b and 1c for an AMIP\_full or AMIP\_noSIC trend (red or blue), or Figure 1d for an AMIP\_SIC trend (green). Time series attributed to sea ice forcing and their linear trends are expanded separately in Figures 2b, 2d, and 2f.

The AMIP trends have a broad maximum warming over  $40^{\circ}$ – $60^{\circ}\text{N}$ , so the tropospheric temperature gradient is weakened toward lower latitudes and strengthened toward higher latitudes, although simulated warming trends over many Arctic grid boxes are significantly smaller than in reanalysis. The 925 and 500 hPa responses associated with sea ice loss (Figures 3g and 3h) are predominantly cooling over midlatitude continents and oceans, whereas warming is significant only at 925 hPa in the western Arctic from the Chukchi Sea to Baffin Bay and in the middle Pacific. The weak Arctic amplification effect due to summer ice loss here is consistent with previous studies [Deser et al., 2010; Screen et al., 2012; Screen et al., 2013; Peings and Magnusdottir, 2014]. Since summer SAT over the Arctic Ocean must remain close to freezing as sea ice melts, turbulent fluxes are weakest and heating influences are limited during the summer. The Arctic warming aloft in the midtroposphere in Figure 3d is mainly driven by greenhouse gas radiative forcing and by SST changes outside the Arctic, indicating enhanced poleward heat transport [Alexeev et al., 2005; Graversen et al., 2008]. This reinforces findings that Arctic warming in the last few decades has been driven by midlatitude and tropical SST warming [Screen et al., 2012; Perlwitz et al., 2015], especially Arctic amplification in summer.



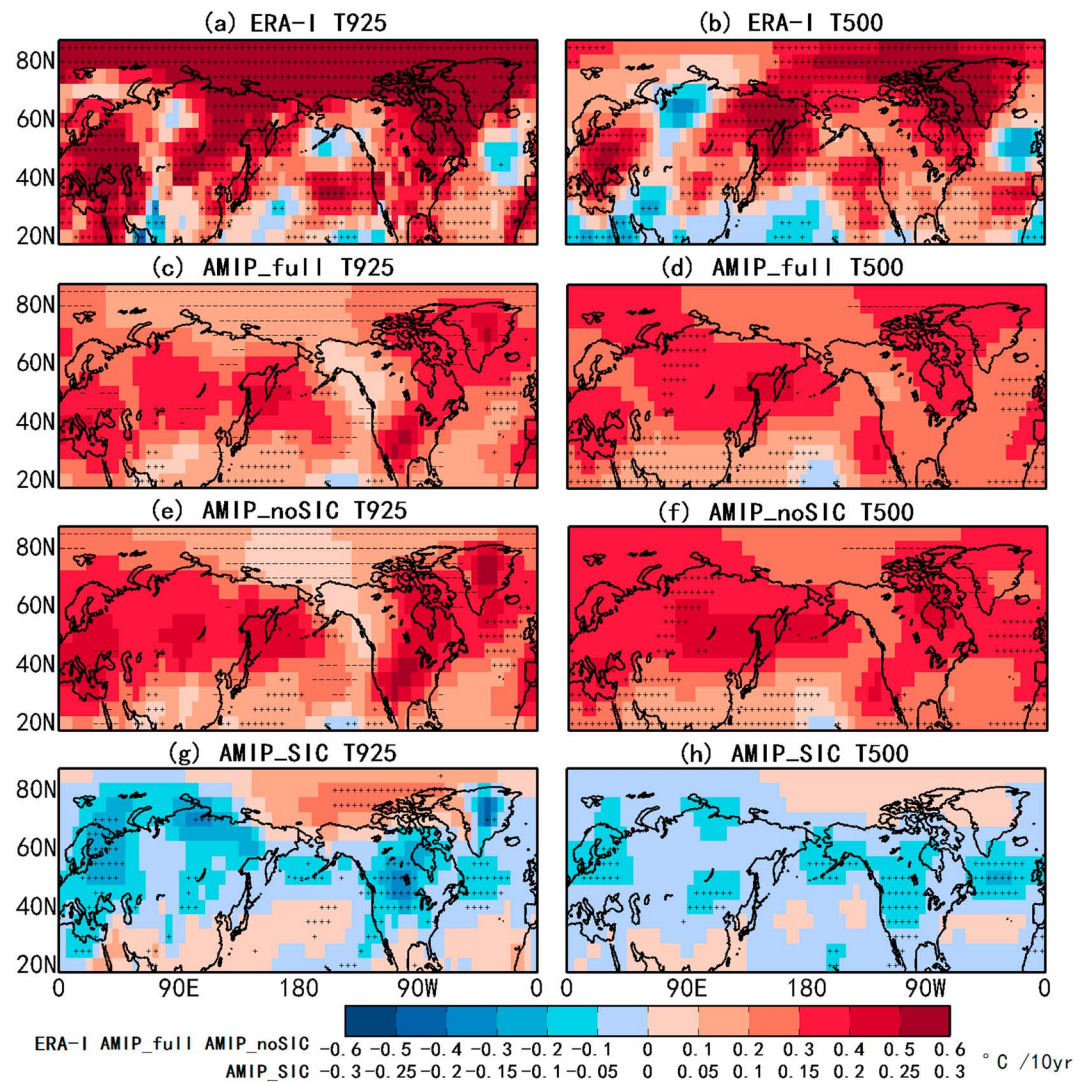


**Figure 3.** The 1979–2012 linear trends of air temperature [ $\text{K} (10 \text{ yr})^{-1}$ ] (a, c, e, and g) at 925 hPa and (b, d, f, and h) 500 hPa, in (Figures 3a and 3b) observations (ERA-Interim reanalysis) and superensemble mean trends in the (Figures 3c and 3d) AMIP\_full and (Figures 3e and 3f) AMIP\_noSIC experiments, and (Figures 3g and 3h) trend component attributed to sea ice forcing, AMIP\_SIC. Plus/minus symbols mark individual grid boxes with significant warming/cooling trends in Figures 3a and 3b, and significantly larger/smaller forced trends than observations in Figures 3c–3f, and significantly different forced trends between the AMIP\_full and AMIP\_noSIC experiments (Figures 3g and 3h) at the 5% significance level.

The JJA 500 hPa geopotential height (Z500) in the AMIP\_full and AMIP\_noSIC runs (Figures 4c and 4e) shows generally increasing trends, as expected from widespread simulated tropospheric warming. Observed reanalysis trend patterns (Figure 4a) are reproduced by the AMIP\_full superensemble (Figure 4c), except for decreasing height trends in the central Atlantic and northern Siberia. The forced trend in Figure 4e, with a broad maximum around 50°N, implies a decreasing height gradient toward lower latitudes leading to a weakened subtropical jet stream, and an increasing height gradient toward higher latitudes with a strengthened polar jet stream. In Figure 4f, the subtropical jet is significantly weakened across southern Eurasia, the Pacific, North America, and the Atlantic, which bears considerable similarity to the reanalysis trend in Figure 4b, indicating that forcings in AMIP\_noSIC have contributed to a weakening summer midlatitude jet in the past decades [Coutou et al., 2015].

The Z500 atmospheric circulation response to sea ice decline resembles a negative summer AO [Ogi et al., 2004] or North Atlantic Oscillation (NAO) pattern over the Atlantic sector (Figure 4g) with positive height anomalies in the Arctic surrounded by negative anomalies through most of the midlatitude NH. In Ogi et al. [2004], a negative summer AO is apparently associated with warming SAT in the Arctic and cool SAT over Eurasia and North

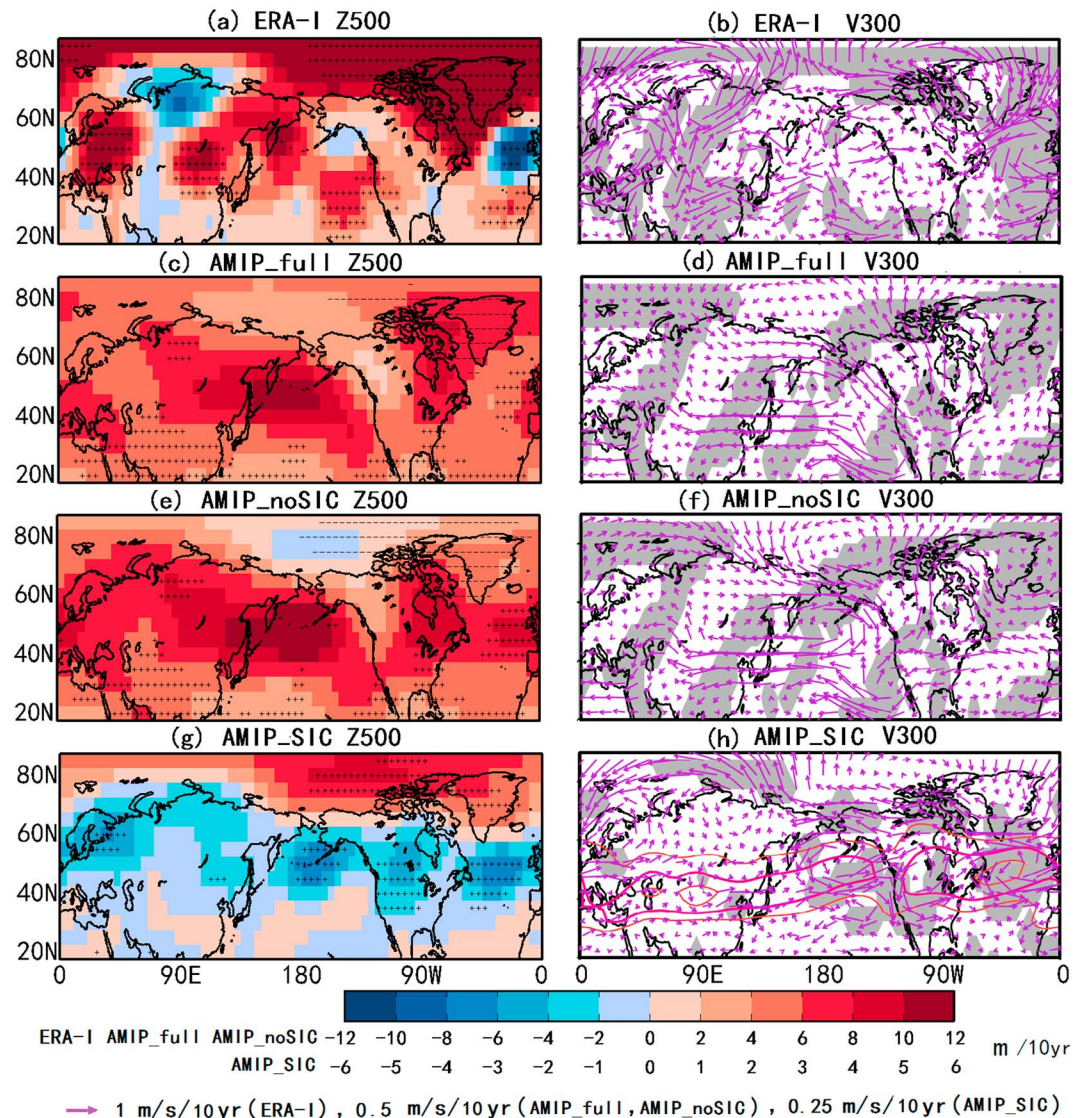


**Figure 4.** The 1979–2012 linear trends of (a, c, e, and g) 500 hPa geopotential height [ $\text{m}/10\text{yr}$ ]<sup>-1</sup> and (b, d, f, and h) 300 hPa wind vectors [ $\text{m}/\text{s}/10\text{yr}$ ]<sup>-1</sup> in (Figures 4a and 4b) observations, superensemble mean trends in the (Figures 4c and 4d) AMIP\_full and (Figures 4e and 4f) AMIP\_noSIC experiments, and (Figures 4g and 4h) trend component attributed to sea ice forcing. In Figure 4h, 300 hPa climatological zonal wind speed  $\geq 10 \text{ m}/\text{s}$  is overplotted (red, interval  $5 \text{ m}/\text{s}$ , thick contour is  $15 \text{ m}/\text{s}$ ). Plus/minus symbols have the same meaning as in Figure 3. Gray shaded areas in Figures 4b, 4d, 4f, and 4h have significant trends of 300 hPa zonal and/or meridional wind speed (Figures 4b and 4h) and significantly different forced trends of 300 hPa zonal and/or meridional wind speed than observations in Figures 4d and 4f at the 5% level.

America. Similar responses are also found at other tropospheric levels (not shown). This suggests that sea ice loss has reduced thickness gradients between the midlatitudes and Arctic and thus weakened the summer polar vortex. The 300 hPa wind response in Figure 4h exhibits a strengthened midlatitude jet stream from East Asia to the middle Atlantic, but weakened upper level zonal winds in the north side of the climatological position of the midlatitude jet stream in the North America and Atlantic sector. Anomalous easterly flows along much of the coastal Arctic and enhanced meridional flows at high-middle latitudes allow Arctic cold air to more frequently reach well into the midlatitudes of northwestern North America, Europe, and northern Russia. Meanwhile, anomalous cyclonic flows over extratropical oceans allow cool maritime air masses to advance more frequently into Europe and western North America. Cold centers of SAT and tropospheric air temperature (Figures 1d, 3g, and 3h) largely collocate with tropospheric lows in Figures 4g and 4h, suggesting that sea ice loss causes relative midlatitude cooling through these circulation changes.



The summer AO index has shown a strong negative trend since 1979 [Wang *et al.*, 2009]. Differences between observed and forced Z500 trends in the AMIP\_full experiment (Figure S3) exhibit a stronger negative summer AO pattern than Figure 4g, suggesting that the observed large negative trend of the summer AO index in the past few decades may be predominantly internally driven. Differences in observed and forced trends in Figures 3 and 4 may be partially explained by this leading mode of atmospheric variability.

#### 4. Conclusions and Discussion

Our results indicate that the hypothesized causality of extreme midlatitude summer weather originating from Arctic sea ice loss [Tang *et al.*, 2014; Overland, 2014] is not supported in simulations with climate models. Screen *et al.* [2013] carried out CAM3 and UM7.3 (the UK-Australian Unified Model version 7.3) atmospheric model experiments for 1979–2009 with no prescribed time-varying forcings except observed Arctic SIC and accompanying Arctic SST variations. Their ensemble mean 925 hPa responses show coherent cooling trends over most midlatitude areas in North America during May–June (MJ) and July–August in the CAM3, but not in UM7.3. The response of summer SAT to the forcing of SIC based on differences between a 2007–2011 low-ice period and a 1996–2005 reference period in atmospheric model HadGEM3 also shows cooling anomalies over Western Europe and eastern North America [Petrie *et al.*, 2015]. Balmaseda *et al.* [2010] evaluate the impact of the 2007 and 2008 observed ice anomalies in the European Centre for Medium-Range Weather Forecasts model and also report a negative AO-like atmospheric response in summer. This cooling response is robust across different models and experiment schemes in our study, as well as in other studies [Screen *et al.*, 2013; Petrie *et al.*, 2015]. A negative AO-like circulation response to sea ice loss here is also consistent with Balmaseda *et al.* [2010]. We conclude that Arctic sea ice loss has partly offset the summer warming in midlatitudes. Such a cooling effect might have reduced the probability of regional severe hot summers since the Arctic sea ice loss has not resulted in significant changes in variance of summer mean surface or tropospheric air temperature (not shown).

Several studies have shown that the simulated response to sea ice loss is model dependent [Screen *et al.*, 2013, 2014; Cohen *et al.*, 2014]. The two models exhibit similar broad patterns of midlatitude cooling but differ considerably in the strength and locations of some regional features (Figure S4). For example, the cooling over Europe is shifted much farther south in ECHAM4 than in CAM4, and cooling over North America is much stronger in CAM4 than in ECHAM5. Over Northern Russia CAM4 shows cooling, but ECHAM5 shows warming. The different spatial patterns of cooling between the models might suggest slightly different causal processes and should be studied further. However, the responses to ice loss (Figures 1d, S4a, and S4b) are much smaller than observed warming trends in Figure 1a, suggesting that Arctic sea ice loss is not the dominant cause of widespread NH land warming since 1979.

Widespread summer NH land and troposphere warming (including Arctic warming aloft in the midtroposphere) is predominantly driven by greenhouse gas radiative forcing and by SST changes outside the Arctic. Detection and attribution studies support an anthropogenic-induced warming of the global ocean since 1979 [Bindoff *et al.*, 2014; Knutson *et al.*, 2013; Chan and Wu, 2015]. The oceanic warming has increased the specific humidity throughout the atmosphere, which warms the continents by increasing downwelling longwave radiation [Compo and Sardeshmukh, 2009; Deser and Phillips, 2009]. The ongoing greenhouse gas buildup and resulting SST warming have also significantly weakened midlatitude zonal winds (Figure 3f) and might have dynamically contributed to more persistent heat waves. Therefore, it is very likely that events such as heat waves in Europe in 2003, Russia in 2010, and the southern United States in 2011 became more extreme due to effects of rising greenhouse gas concentrations [Rahmstorf and Coumou, 2011; Stott *et al.*, 2004] but were not further prolonged and intensified by Arctic sea ice decline and resulting Arctic amplification.

#### References

- Alexeev, V., P. Langen, and J. Bates (2005), Polar amplification of surface warming on an aquaplanet in ghost forcing experiments without sea ice feedbacks, *Clim. Dyn.*, *24*, 655–666.
- Balmaseda, M. A., L. Ferranti, F. Molteni, and T. N. Palmer (2010), Impact of 2007 and 2008 Arctic ice anomalies on the atmospheric circulation: Implications for long-range predictions, *Q. J. R. Meteorol. Soc.*, *136*, 1655–1664.
- Barnes, E. A. (2013), Revisiting the evidence linking Arctic amplification to extreme weather in midlatitudes, *Geophys. Res. Lett.*, *40*, 4734–4739, doi:10.1002/grl.50880.
- Barnes, E. A., and J. A. Screen (2015), The impact of Arctic warming on the midlatitude jet-stream: Can it? Has it? Will it? *WIREs Clim Change*, *6*, 277–286.

#### Acknowledgments

We acknowledge ESRL for producing and making available model outputs ([www.esrl.noaa.gov/psd/repository/](http://www.esrl.noaa.gov/psd/repository/)). NOAA Merged Air Land and SST Anomalies data are provided by the NOAA/OAR/ESRL PSD, Boulder, Colorado, USA, from their Web site at <http://www.esrl.noaa.gov/psd/>. We are grateful for the insightful and constructive comments from two anonymous reviewers. This work is funded by the National Key Scientific Research Plan of China (grant 2012CB956002) and the National Natural Science Foundation of China (grant 41075052). This work is also supported by the Jiangsu Collaborative Innovation Center for Climate Change and CMA-NJU Joint Laboratory for Climate Prediction Studies.

- Barnes, E. A., E. Dunn-Sigouin, G. Masato, and T. Woollings (2014), Exploring recent trends in Northern Hemisphere blocking, *Geophys. Res. Lett.*, **41**, 638–644, doi:10.1002/2013GL058745.
- Bindoff, N. L., et al. (2014), Detection and attribution of climate change: From global to regional, in *Climate Change 2013: The Physical Science Basis*, edited by T. F. Stocker et al., pp. 867–952, Cambridge Univ. Press, Cambridge, U. K.
- Chan, D., and Q. Wu (2015), Attributing observed SST trends and subcontinental land warming to anthropogenic forcing during 1979–2005, *J. Clim.*, **28**, 3152–3170.
- Cohen, J., et al. (2014), Recent Arctic amplification and extreme mid-latitude weather, *Nat. Geosci.*, **7**, 627–637.
- Compo, G. P., and P. D. Sardeshmukh (2009), Oceanic influences on recent continental warming, *Clim. Dyn.*, **32**, 333–342.
- Coumou, D., and S. Rahmstorf (2012), A decade of weather extremes, *Nat. Clim. Change*, **2**, 491–496.
- Coumou, D., V. Petoukhov, S. Rahmstorf, S. Petri, and H. J. Schellnhuber (2014), Quasi-resonant circulation regimes and hemispheric synchronization of extreme weather in boreal summer, *Proc. Natl. Acad. Sci. U.S.A.*, **111**, 12,331–12,336.
- Coumou, D., J. Lehmann, and J. Beckmann (2015), The weakening summer circulation in the Northern Hemisphere mid-latitudes, *Science*, **348**, 324–327.
- Dee, D. P., et al. (2011), The ERA-Interim reanalysis: Configuration and performance of the data assimilation system, *Q. J. R. Meteorol. Soc.*, **137**, 553–597.
- Deser, C., and A. S. Phillips (2009), Atmospheric circulation trends, 1950–2000: The relative roles of sea surface temperature forcing and direct atmospheric radiative forcing, *J. Clim.*, **22**, 396–413.
- Deser, C., R. Tomas, M. Alexander, and D. Lawrence (2010), The seasonal atmospheric response to projected Arctic sea ice loss in the late twenty-first century, *J. Clim.*, **23**, 333–351.
- Deser, C., R. A. Tomas, and L. Sun (2015), The role of ocean–atmosphere coupling in the zonal-mean atmospheric response to Arctic sea ice loss, *J. Clim.*, **28**, 2168–2186.
- Francis, J. A., and S. J. Vavrus (2012), Evidence linking Arctic amplification to extreme weather in mid-latitudes, *Geophys. Res. Lett.*, **39**, L06801, doi:10.1029/2012GL051000.
- Francis, J. A., and S. J. Vavrus (2015), Evidence for a wavier jet stream in response to rapid Arctic warming, *Environ. Res. Lett.*, **10**, 014005.
- Francis, J. A., W. Chan, D. J. Leathers, J. R. Miller, and D. E. Veron (2009), Winter Northern Hemisphere weather patterns remember summer Arctic sea ice extent, *Geophys. Res. Lett.*, **36**, L07503, doi:10.1029/2009GL037274.
- Graversen, R., T. Mauritsen, M. Tjernström, E. Källén, and G. Svensson (2008), Vertical structure of recent Arctic warming, *Nature*, **451**, 53–56.
- Honda, M., J. Inue, and S. Yamane (2009), Influence of low Arctic sea-ice minima on anomalously cold Eurasian winters, *Geophys. Res. Lett.*, **36**, L08707, doi:10.1029/2008GL037079.
- Kim, B., S.-W. Son, S.-K. Min, J.-H. Jeong, S.-J. Kim, X. Zhang, T. Shim, and J.-H. Yoon (2014), Weakening of the stratospheric polar vortex by Arctic sea-ice loss, *Nat. Commun.*, **5**, 4646, doi:10.1038/ncomms5646.
- Knutson, T. R., F. Zeng, and A. T. Wittenberg (2013), Multimodel assessment of regional surface temperature trends, *J. Clim.*, **26**, 8709–8743.
- Liu, J., J. A. Curry, H. Wang, M. Song, and R. Horton (2012), Impact of declining Arctic sea ice on winter snow, *Proc. Natl. Acad. Sci. U.S.A.*, **109**, 4074–4079.
- Magnusdottir, G., C. Deser, and R. Saravanan (2004), The effects of North Atlantic SST and sea-ice anomalies on the winter circulation in CCM3. Part I: Main features and storm track characteristics of the response, *J. Clim.*, **17**, 857–876.
- Neale, R., J. Richter, S. Park, P. H. Lauritzen, S. J. Vavrus, P. J. Rasch, and M. Zhang (2013), The mean climate of the Community Atmosphere Model (CAM4) in forced SST and fully coupled experiments, *J. Clim.*, **26**, 5150–5168.
- Ogi, M., K. Yamazaki, and Y. Tachibana (2004), The summertime annular mode in the Northern Hemisphere and its linkage to the winter mode, *J. Geophys. Res.*, **109**, D20114, doi:10.1029/2004JD004514.
- Orsolini, Y., R. Senan, R. Benestad, and A. Melsom (2012), Autumn atmospheric response to the 2007 low Arctic sea ice extent in coupled ocean–atmosphere hindcasts, *Clim. Dyn.*, **38**, 2437–2448.
- Overland, J. E. (2014), Long-range linkage, *Nat. Clim. Change*, **4**, 11–12.
- Overland, J., and M. Wang (2010), Large-scale atmospheric circulation changes are associated with the recent loss of Arctic sea ice, *Tellus*, **62A**, 1–9.
- Palmén, E., and C. W. Newton (1969), *Atmospheric Circulation Systems*, Int. Geophys. Ser., vol. 13, Academic Press, New York.
- Peings, Y., and G. Magnusdottir (2014), Response of the wintertime Northern Hemisphere atmospheric circulation to current and projected Arctic sea ice decline: A numerical study with CAM5, *J. Clim.*, **27**, 244–264.
- Perlitz, J., M. Hoerling, and R. Dole (2015), Arctic tropospheric warming: Causes and linkages to lower latitudes, *J. Clim.*, **28**, 2154–2167.
- Petoukhov, V., S. Rahmstorf, S. Petri, and H. J. Schellnhuber (2013), Quasiresonant amplification of planetary waves and recent northern hemisphere weather extremes, *Proc. Natl. Acad. Sci. U.S.A.*, **110**, 5336–5341.
- Petrie, R. E., L. C. Shaffrey, and R. T. Sutton (2015), Atmospheric response in summer linked to recent Arctic sea ice loss, *Q. J. R. Meteorol. Soc.*, **141**, 2070–2076, doi:10.1002/qj.2502.
- Rahmstorf, S., and D. Coumou (2011), Increase of extreme events in a warming world, *Proc. Natl. Acad. Sci. U.S.A.*, **108**, 17,905–17,909.
- Roeckner, E., et al. (2003), The atmospheric general circulation model ECHAM5. Part I: Model description Max Planck Institute for Meteorology Tech. Rep. 349, 127 pp.
- Screen, J. A., C. Deser, and I. Simmonds (2012), Local and remote controls on observed Arctic warming, *Geophys. Res. Lett.*, **39**, L10709, doi:10.1029/2012GL051598.
- Screen, J. A., I. Simmonds, C. Deser, and R. Tomas (2013), The atmospheric response to three decades of observed Arctic sea ice loss, *J. Clim.*, **26**, 1230–1248.
- Screen, J. A., C. Deser, I. Simmonds, and R. Tomas (2014), Atmospheric impacts of Arctic sea ice loss, 1979–2009: Separating forced change from atmospheric internal variability, *Clim. Dyn.*, **43**, 333–344.
- Serreze, M. C., A. P. Barrett, J. C. Stroeve, D. N. Kindig, and M. M. Holland (2009), The emergence of surface-based Arctic amplification, *Cryosphere*, **3**, 11–19.
- Smith, T. M., R. W. Reynolds, T. C. Peterson, and J. Lawrimore (2008), Improvements to NOAA's historical merged land-ocean surface temperature analysis (1880–2006), *J. Clim.*, **21**, 2283–2293.
- Stott, P. A., D. A. Stone, and M. R. Allen (2004), Human contribution to the European heatwave of 2003, *Nature*, **432**, 610–614.
- Stroeve, J. C., M. C. Serreze, M. M. Holland, J. E. Kay, J. Malanik, and A. P. Barrett (2012), The Arctic's rapidly shrinking sea ice cover: A research synthesis, *Clim. Change*, **110**, 1005–1027.
- Strong, C., G. Magnusdottir, and H. Stern (2010), Observed feedback between winter sea ice and the North Atlantic Oscillation, *J. Clim.*, **22**, 6021–6032.



- Tang, Q., X. Zhang, and J. A. Francis (2014), Extreme summer weather in northern mid-latitudes linked to a vanishing cryosphere, *Nat. Clim. Change*, **4**, 45–50.
- Trenberth, K., M. C. Serreze, M. M. Holland, J. E. Kay, J. Malanik, and A. P. Barrett (2014), Seasonal aspects of the recent pause in surface warming, *Nat. Clim. Change*, **4**, 911–916.
- Vaughan, D. G., et al. (2014), Observations: Cryosphere, in *Climate Change 2013: The Physical Science Basis*, edited by T. F. Stocker et al., pp. 317–382, Cambridge Univ. Press, Cambridge, U. K.
- Wallace, J. M., I. M. Held, D. W. J. Thompson, K. E. Trenberth, and J. E. Walsh (2014), Global warming and winter weather, *Science*, **343**, 729–730.
- Wang, J., J. Zhang, E. Watanabe, M. Ikeda, K. Mizobata, J. E. Walsh, X. Bai, and B. Wu (2009), Is the Dipole Anomaly a major driver to record lows in Arctic summer sea ice extent? *Geophys. Res. Lett.*, **36**, L05706, doi:10.1029/2008GL036706.
- Wu, Q., and X. Zhang (2010), Observed forcing-feedback processes between Northern Hemisphere atmospheric circulation and Arctic sea ice coverage, *J. Geophys. Res.*, **115**, D14119, doi:10.1029/2009JD013574.